

NUMERICAL SIMULATION OF THE RESTART PROBLEM FOR THIXOTROPIC FLUIDS

Leandro de Souza Alencar, leandro.s.alencar@gmail.com

PETROBRAS E&P-PRESAL/CT/EEIP, Rio de Janeiro, RJ 20031-170, Brazil.

Mônica Naccache, naccache@puc-rio.br

PUC-RJ Mechanical Engineering Department, Rua Marquês de São Vicente 225, Rio de Janeiro, RJ 22453-900, Brazil.

Abstract. *Many industrial applications involve the transport of complex fluids, such as paint, paper and oil. Especially for the oil production in ultra-deep water fields, the transport of oil with high paraffins content can create some difficulties. The produced fluid cools down inside the pipeline when the production stops and the paraffin crystals form an interlocking gel-like structure. The knowledge of the thixotropic behaviour of the produced fluid together with the simulation capacity to solve the restart phenomenon enables the economical design of pumps and lines with reasonable precision and size to break the gel. Several mathematical models exist in the literature that tries to explain this phenomenon, including scalar models in which the structure of the fluid is represented by one single parameter. This type of model is simple and with the most practical use. So it was chosen for this thesis. A non-linear first order differential equation is used for the thixotropic evolution relation and must be coupled with the standard transport equations. The use of a numerical simulator that can solve this problem gives the engineer the tool required to solve for any geometry the restart problem. The issue lies within the simulator capacity to represent the thixotropic behaviour and if it has the confiability required for industrial applications. In this thesis the algorithm developed to implement the thixotropic simulation within the CFD commercial tool Fluent© is presented for a purely viscous incompressible fluid. Two restart cases are discussed in detail and the effect of the inlet boundary condition is presented together with a relationship between the restart time and the inlet pressure for different thixotropic conditions. A comparison between the simulation of the restart problem and some experimental data shows that the expected behaviour is achieved with good qualitative similarities. In conclusion, the results herein presented prove the potential use of CFD with thixotropic fluids enabling the optimized design of production systems.*

Keywords: *Non-Newtonian flow, Thixotropy, CFD, Restart problem*

1. INTRODUCTION

Many industrial applications involve the transport of complex fluids, such as paint, paper and oil. Especially for the oil production in ultra-deep water fields, the transport of oil with high paraffin content can create some difficulties. The produced fluid cools down inside the pipeline when the production stops and the paraffin crystals form an interlocking gel-like structure (Lima, 2015). This structure changes the rheology of the system, which may result in a gel-like fluid with viscoplastic and thixotropic behavior with a high yield stress. Because of that, the flow restart requires a high pressure in order to break the interlocked structure of the cold fluid.

Thixotropic behavior is characterized by having a time-dependent structure breakdown or build-up behavior represented, for example, with a viscosity increase or decrease (Barnes, 1997). In the absence of shear, the fluid gels and exhibits a yield stress. Most CFD software do not have a thixotropy model implemented, since there is still a discussion in the literature regarding the constitutive equation to model this behavior, which is still not fully understood. Moreover, the highly complex behavior of the equations proposed so far is also an issue. The motivation of this study is to show how CFD can be used help in the understanding of the thixotropic behavior by implementing a series of computer routines and to test and compare the effects of different boundary conditions in the simulation results.

The approach adopted in this work is to model the thixotropic behavior through a modified equation for viscosity, with the addition of one more transport equation to be solved to take into account the thixotropy effect through the use of a structure parameter that gives the structure level of the fluid. Several mathematical models exist in the literature to explain this phenomenon, including scalar models in which the fluid structure is represented by one single parameter (Mujumdar, 2002). This type of model is simple and with the most practical use. In this work, we use the constitutive model proposed by de Souza Mendes (2009), which is more robust, and able to predict the main rheological characteristics of thixotropic materials. However, the applied methodology can be used in any scalar model.

To validate the numerical modeling, the restart problem in a pipe is modeled using the Fluent© commercial software. The thixotropic fluid is initially at rest, in its highest structured state, and suddenly a constant pressure source is applied at the inlet. The mean velocity is measured at the outlet to compare with some experimental data. The 2-D model also allows the visualization of the structure parameter in a spatial distribution to help a detailed inspection of the restart process.

2. PROBLEM DESCRIPTION

The main equations governing the flow, mass and momentum conservation, are presented together with the constitutive equation used for the structure parameter. Then the problem is simplified by taking into consideration the assumptions adopted herein. The boundary conditions and the overall simulation configuration are shown at the end of this section.

2.1 Mathematical Equations

Equation (1) and (2) shows the momentum and continuity equation respectively for a transient isothermal flow of an incompressible fluid in a 2-D environment without relevant gravitational force.

$$0 = \frac{\partial u_i}{\partial x_i} \quad (1)$$

$$\rho \frac{\partial u_i}{\partial t} + \rho u_i \frac{\partial u_i}{\partial x_i} = \frac{\partial \pi_{ii}}{\partial x_i} + \frac{\partial \pi_{ij}}{\partial x_j} \quad (2)$$

where ρ is the specific gravity, u_i the velocity in the x_i direction and π_{ij} the stress tensor.

The stress tensor can assume the form presented in Eq. (3) for purely viscous fluids, where p is the pressure. The radial direction is represented with the letter r , the longitudinal direction with x and the apparent viscosity with η .

$$\pi_{ij} = \begin{bmatrix} -p & 0 \\ 0 & -p \end{bmatrix} + \eta \begin{bmatrix} 0 & \frac{\partial u_x}{\partial r} + \frac{\partial u_r}{\partial x} \\ \frac{\partial u_x}{\partial r} + \frac{\partial u_r}{\partial x} & 0 \end{bmatrix} \quad (3)$$

The viscosity function is a function of the fluid structure level and is given by the thixotropy model proposed by de Souza Mendes (2009). This behavior should follow a relation in which the apparent viscosity η tends to a maximum value η_0 when the fluid is completely structured and to a minimum value η_∞ when unstructured, as shown in Eq. (4). The fluid structure level can be represented by a parameter λ that varies from one, associated with a completely structured state, to zero, for completely unstructured state.

$$\eta = \left(\frac{\eta_0}{\eta_\infty} \right)^\lambda \eta_\infty \quad (4)$$

The structure parameter λ is obtained through the evolution equation shown in Eq. (5) (de Souza Mendes, 2009). This model depends only in four parameters: three constants (t_{eq} , b and a) and the structure parameter in the equilibrium state, λ_{eq} .

$$\frac{D\lambda}{Dt} = \frac{1}{t_{eq}} \left[(1 - \lambda)^a - (1 - \lambda_{eq})^a \left(\frac{\lambda}{\lambda_{eq}} \right)^b \right] \quad (5)$$

The structure parameter in equilibrium, λ_{eq} , can be obtained rearranging Eq. (4) and substituting η with the viscosity flow curve obtained experimentally. For a viscoplastic material behavior, a regularized model should be used for the viscosity function to avoid numerical problems in the simulation. Examples of this type of model are proposed by Papanastasiou (1999) and by de Souza Mendes (2004). The model proposed by the latter is presented in Eq. (6), and was the one used in this work.

$$\eta = \left(m\dot{\gamma}^{n-1} + \frac{\tau_0}{\dot{\gamma}} \right) \left(1 - e^{-\eta_0 \dot{\gamma} / \tau_0} \right) + \eta_\infty \quad (6)$$

where m and n are constants obtained with experimental data matching, τ_0 the yield stress, and $\dot{\gamma}$ the strain rate.

Equations (1), (2) and (5) have to be iteratively solved by the numerical simulator with the finite volume method. However, for Eq. (5) to be solved the total derivative term must be separated in its transient and advective form. The source term must also have a linear relation with the independent variable given by λ . A first order Taylor expansion is used in the source term following the recommended procedure proposed by Patankar (1980).

Figure 1 summarizes the equations used and its dependencies to highlight the iterative process needed to solve the flow problem. The stress tensor in Eq. (2) is replaced by its complete form given by Eq. (3), with the viscosity function given by Eq. (4). Equation (5) was expanded in order to show the transient and the advective terms.

$$\begin{aligned}
 & 0 = \frac{\partial \rho u_i}{\partial x_i} \quad \text{Ref. Eq. (1)} \\
 & \rho \frac{\partial u_i}{\partial t} + \rho u_i \frac{\partial u_i}{\partial x_i} = -\frac{\partial p}{\partial x_i} + \frac{\partial}{\partial x_j} \left[\left(\frac{\eta_0}{\eta_\infty} \right)^\lambda \eta_\infty \frac{\partial u_i}{\partial x_j} \right] \quad \text{Ref. Eq. (2)/(3)/(4)} \\
 & \frac{d\lambda}{dt} = \frac{1}{t_{eq}} \left[(1-\lambda)^a - (1-\lambda_{eq})^a \left(\frac{\lambda}{\lambda_{eq}} \right)^b \right] \quad \text{Ref. Eq. (5)} \\
 & \lambda_{eq} = (\ln \eta_{eq} - \ln \eta_\infty) / (\ln \eta_0 - \ln \eta_\infty) \quad \text{Ref. Eq. (4)} \\
 & \eta_{eq} = \left(m \dot{\gamma}^{n-1} + \frac{\tau_0}{\dot{\gamma}} \right) (1 - e^{-\eta_0 \dot{\gamma} \tau_0}) + \eta_\infty \quad \text{Ref. Eq. (6)}
 \end{aligned}$$

Figure 1. Equations summary with the coupling parameter highlighted

2.2 Configurations and Boundary Conditions

The CFD tool Fluent© allows the user to implement different procedures that can be accessed by the program at each simulation. The viscosity function (Eq. (4)) and the thixotropy evolution equation (Eq. (6)) are represented by different procedures. Especially for the thixotropy, three procedures are required for each one of the source, transient and advective terms. The procedures were written in C programming language.

A segment of a pipe with a length-to-diameter ratio of 40 was modeled as represented by the gray area in Fig. 2. The velocity measurements are taken near the outlet. The pressure-based solver was used for the transient axisymmetric model, with the PISO algorithm for the pressure-velocity coupling. The continuity equation was discretized with the power-law method and the momentum and evolution equation were solved with the second order discretization method.

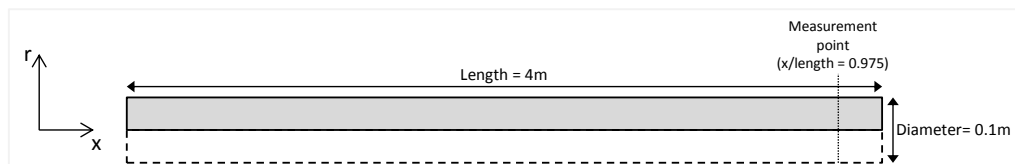


Figure 2. Problem description

The following boundary conditions for the flow domain were used:

- At the inlet:
 - constant pressure
 - constant or zero axial derivative for the structure parameter
- At the wall: no slip condition for velocity
- Along the axis of symmetry: axisymmetric condition for velocity, pressure and structure parameter
- At the outlet:
 - constant pressure
 - zero axial derivative for the structure scalar

The system initial condition is of zero velocity and the structure parameter λ for the whole flow domain is considered equal to one (fluid completely structured, with maximum viscosity of η_0). When the residual of the system of equations was less than 10^{-6} , convergence was considered to have been achieved by the simulation.

Different mesh refinements were tested with a linear thixotropic model. The average velocity compared with average velocity of the most refined mesh and the average difference between each cell regarding this refined mesh was obtained, as shown by Fig. 3. Mesh M5 was chosen because of its relatively low error compared with the refined mesh that has 10 times more cells.

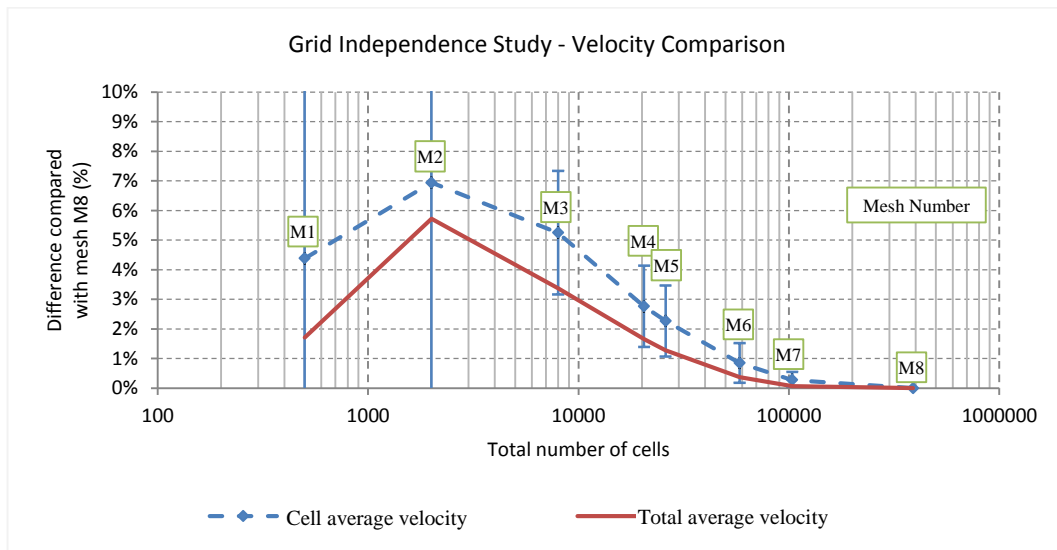


Figure 3. Grid independence study

3. RESULTS

3.1 Start-up Scenario with Boundary Condition Sensibility

Two boundary inlet conditions for the structure parameter were tested. First, a zero axial derivative was imposed, which would correspond to a fully developed Dirichlet condition for λ . Secondly, a Neumann boundary condition for λ was used for the inlet to simulate a pre-sheared condition as would occur after a pump, for instance.

The pressure applied in each case is different so the measured velocity would be approximately the same in both cases. The breakdown of the structure decreases the viscosity to a point where the strain is high enough to induce flow, causing a delay in the restart of the system, as shown in Fig. 4. As the structure breaks, the velocity increases until steady-state is achieved.

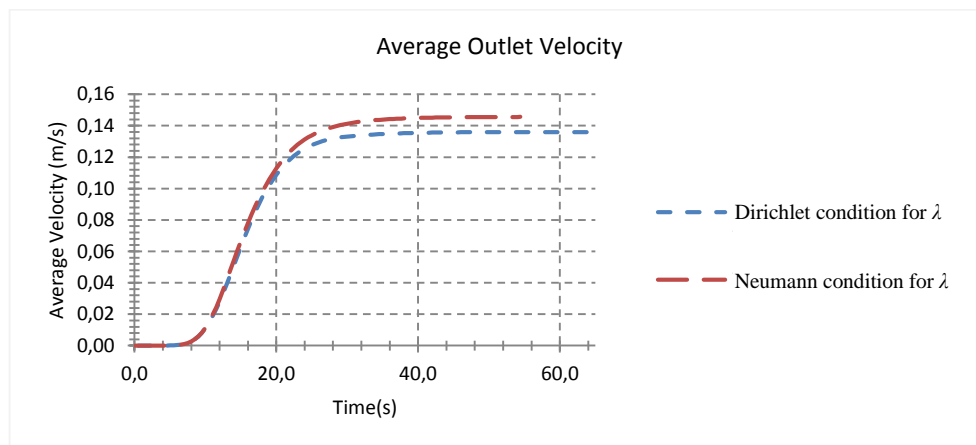


Figure 4. Average velocity obtained for two inlet boundary condition for λ

Figure 5 gives the spatial distribution of the structure parameter λ with respect of time for the Dirichlet boundary condition of λ . In the beginning the system is approximately at its rest state and the fluid structure is at its maximum, with λ equal to one and the viscosity equal to η_0 .

Because the fluid behaves like a high viscosity liquid ($\eta = \eta_0$) for any strain, immediately after the pressure is applied the flow starts, though with almost zero velocity. That is the reason why in Fig. 5A the structure parameter is less than one near the wall, but the measured velocity in Fig. 4 is apparently zero.

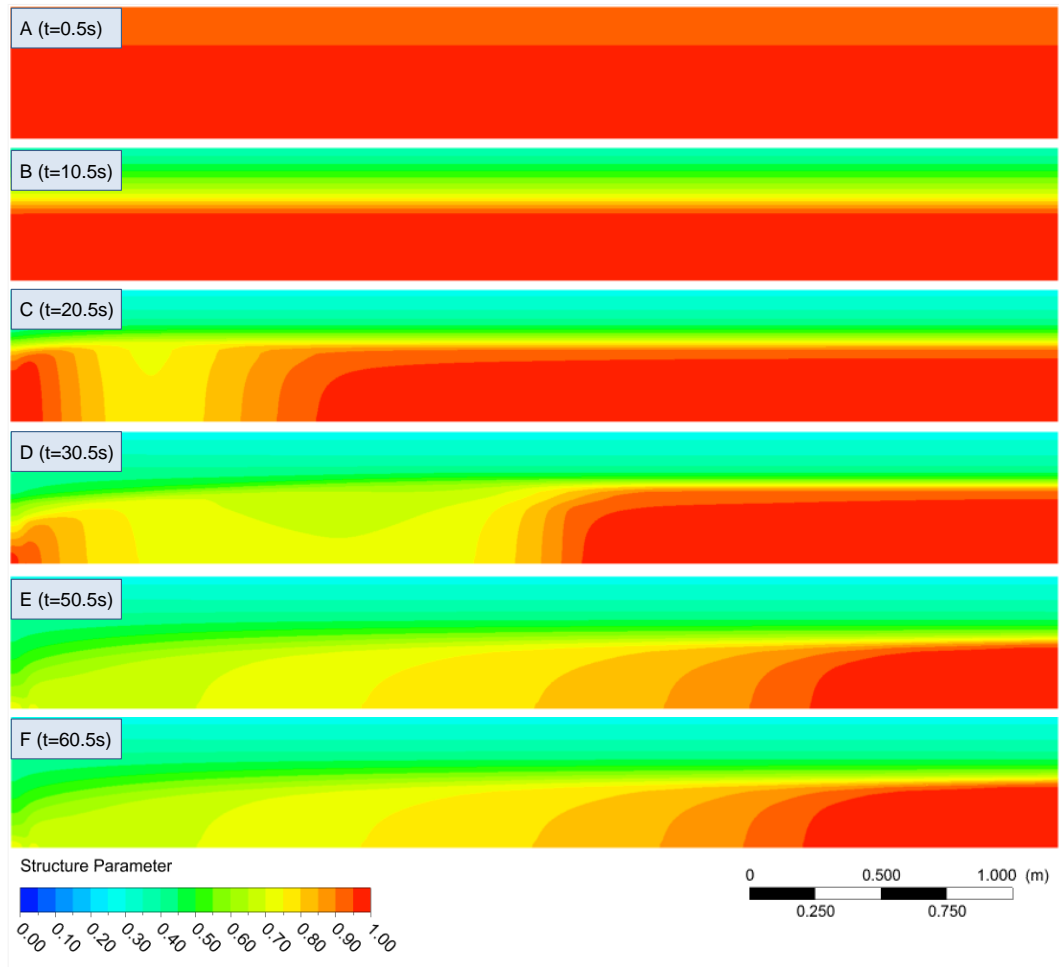


Figure 5. Spatial distribution of λ for Dirichlet boundary condition

A disturb in the structure distribution is observed in Fig. 5C near the inlet of the system. As time passes and with the propagation to the outlet this disturbance is smoothed out until it reaches a developed condition near the exit. Comparison of Figs. 5E and 5F shows that the system reached steady state at 50.5 seconds.

When a Neumann condition is used for λ no disturbance of the kind reported above (Fig. 5C) was observed. A value of 0.2 was arbitrarily chosen for λ at the inlet in Fig. 6. As the time passes, from Fig. 6A to 6F, it is clear that the fluid enters the system until it fills the entire pipe and the structure parameter develops from the inlet value ($\lambda=0.2$) up to a steady state condition near the outlet. The same behavior of the structure parameter distribution in Fig. 5 is observed in Fig. 6 near the outlet boundary.

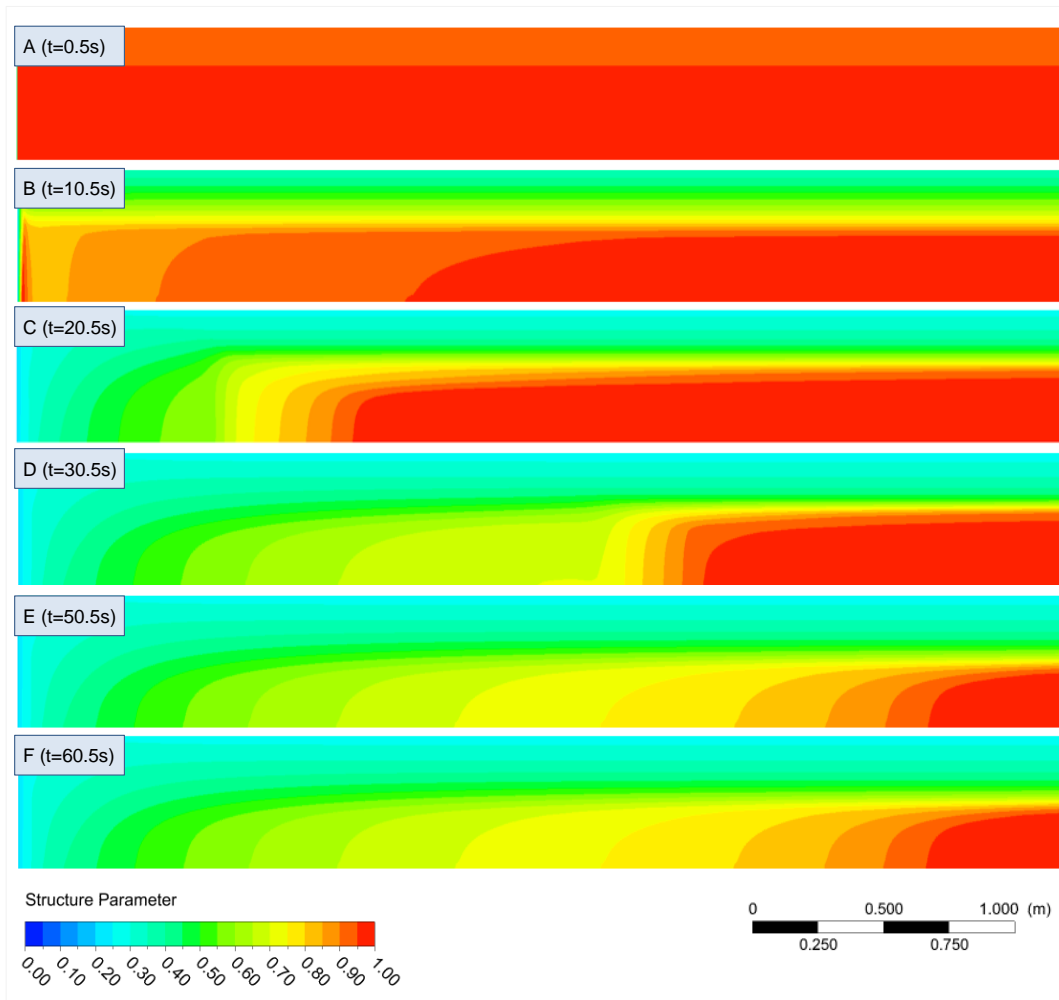


Figure 6. Spatial distribution of λ for Neumann boundary condition

The evolution of λ with time is similar for both simulations shown (Fig. 5 and Fig. 6). In the first seconds the fluid is uniformly broken for both scenarios and the velocity is approximately zero (see boxed area in Fig. 7). After a while, the structure level decays, the fluid velocity increases, and structure λ evolves along the axis until steady state (see arrow in Fig. 7). Although the inlet boundary conditions change the solution near the boundary, they are not relevant for the final results in terms of velocity and time to restart the system.

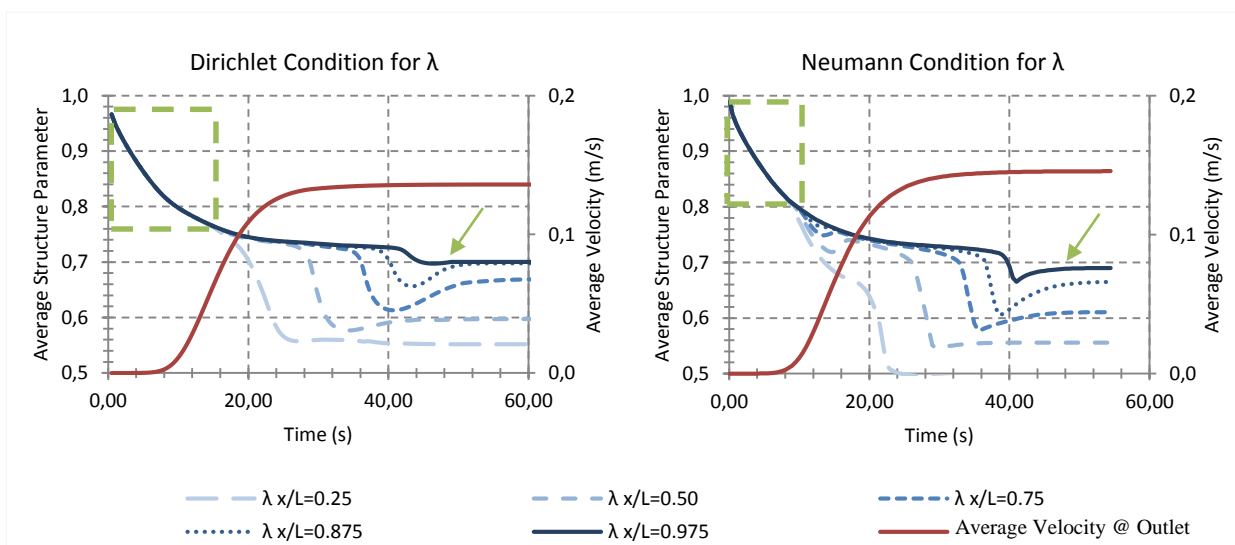


Figure 7. Structure parameter λ averaged in the radial direction at different positions along the axis and average velocity near the outlet for both inlet boundary conditions tested

3.2 Comparison with Experimental Data

Experimental data were used to compare and validate the simulation results. The experimental data presented in this section were obtained by Moisés (2016) through an horizontal acrylic pipe, with approximately 4 meters long and internal diameter of 19mm. The velocity is measured with an ultrasound doppler velocimetry located outside the pipe near the outlet. The fluid rheological properties were the same as the ones used in the simulation herein presented. However, the thixotropic constants of Eq. (6) were not obtained experimentally so they were arbitrarily chosen for the simulations.

A pressure step is applied starting the measurement of the velocity. Three steps of different magnitude were applied. Comparison of the average velocity for the experimental data and simulated results is presented in Fig. 8 and shows a similar qualitative behavior.

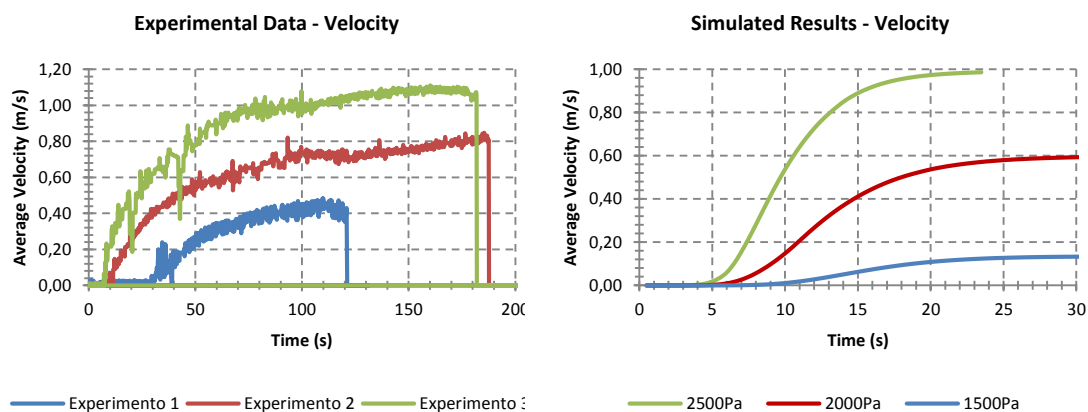


Figure 8. Average velocity for the experimental and simulated cases for three different pressure steps

4. CONCLUSIONS

The methodology and algorithm developed to analyze the thixotropic fluid behavior in a commercial CFD package successfully represented the expected behavior. The results presented show the possibility to simulate the restart problem for engineering applications as long as enough rheological data is available. This allows the optimal design of systems that carries complex fluids with minimum risks. In conclusion, a full analysis of the restart phenomenon for thixotropic fluids was made possible in a full 2-D straight pipe simulation that could easily be extrapolated to any geometry.

5. ACKNOWLEDGEMENTS

The authors are indebted to CNPq, CAPES and PETROBRAS S.A for the financial support.

6. REFERENCES

- Barnes, H. A., 1997. "Thixotropy - a review," *Journal of Non-Newtonian Fluid Mechanics*, vol. 70, pp. 1-33.
- de Souza Mendes, P. R., 2009. "Modeling the thixotropic behavior of structured fluids," *Journal of Non-Newtonian Fluid Mechanics*, vol. 164, pp. 66-75.
- Lima, D. D. S., 2015. Startup Flow of Gelled Crudes after a Shutdown Comparison between Simulations and Experimental Data. Master thesis, Pontifícia Universidade Católica do Rio de Janeiro, Departamento de Engenharia Mecânica, Rio de Janeiro, RJ, Brazil.
- Moisés, G. V. L., 2016. Yield Stress and Thixotropy Effects of Non-Newtonian Fluids in Horizontal Pipe Flows, Ph.D. thesis, Pontifícia Universidade Católica do Rio de Janeiro, Departamento de Engenharia Mecânica, Rio de Janeiro, RJ, Brazil.
- Mujumdar, A., Beris, A. N., and Metzner, A. B., 2002. "Transient Phenomena in Thixotropic Systems," *Journal of Non-Newtonian Fluid Mechanics*, vol. 102, pp. 157-178.
- Patankar, S. V., 1980. *Numerical Heat Transfer and Fluid Flow*. W. Minkowycz & E. M. Sparrow, New York

7. RESPONSIBILITY NOTICE

The authors are the only responsible for the printed material included in this paper.